Polymer Science, Ser. A, Vol. 40, No. 8, 1998, pp. 826–834. Translated from Vysokomolekulyarnye Soedineniya, Ser. A, Vol. 40, No. 8, 1998, pp. 1324–1333.




# Mechanism of Spin and Charge Transport in Poly(aniline)[1]

**V. I. Krinichnyi*, S. D. Chemerisov**, and Ya. S. Lebedev†****

* *Institute of Problems of Chemical Physics, Russian Academy of Sciences, p/o Chernogolovka, Moscow oblast, 142432 Russia*

** *Semenov Institute of Chemical Physics, Russian Academy of Sciences, ul. Kosygina 4, Moscow, 117977 Russia*

Received December 16, 1997;
Revised Manuscript Received February 11, 1998

**Abstract**—Spin dynamics and the conductivity mechanism in poly(aniline) samples with different doping levels were studied by the conductometry and multifrequency EPR techniques. In the neutral polymer, the charge transport occurs predominantly through interchain transfer by hopping between pinned and mobile small polarons. A slight doping of the polymer leads to an isoenergetic charge transfer between the polaron and bipolaron states according to the Kivelson theory. Ultimately high doping of poly(aniline) leads to the formation of highly conducting quasi-three-dimensional clusters. In the low-temperature range, the charge transfer in these clusters proceeds by the mechanism of interchain tunneling and correlates with macromolecular librations of the polymer chain. At high temperatures, the microconductivity of the clusters is determined by the scattering of electrons on the optical lattice phonons.

## INTRODUCTION

Electronic and magnetic properties of quasi-one-dimensional ($1D$) organic semiconductors have been extensively studied in recent years [1, 2]. The charge transfer in the organic polymeric semiconductors, in contrast to the classical semiconductors, is mediated by nonlinear topological excitations, such as solitons in *trans*-poly(acetylene) and polaron–bipolaron pairs in poly(*p*-phenylene) and some other polymeric semiconductors [3, 4]. Special conducting properties of the organic polymeric semiconductor are largely determined by the dynamics of these charge carriers.

The macroscopic conductivity of a polymer depends on the level of doping $y$ (the number of dopant molecules per polymer repeat unit) and is affected by superposition of various electron transfer processes [5]. Poly(aniline), unlike *trans*-poly(acetylene), poly(*p*-phenylene), and other similar organic polymeric semiconductors, contains nitrogen atoms in the conjugation chain. In addition, the benzene rings of aniline monomers are capable of rotating about the principal $x$-axis of the polymer backbone [6]. These structural features account for the considerable difference in the properties between poly(aniline) and other organic polymeric semiconductors. Usually, the polymer occurs in two forms, comprising a mixture of emeraldin base (EB)

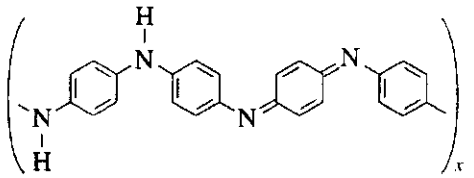

and emeraldin salt (ES)

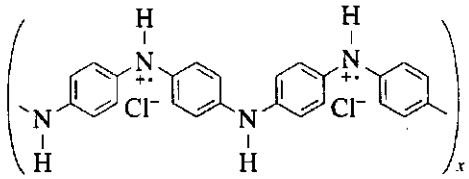

Upon doping, the nonconducting EB form of the polymer transforms into ES, which is accompanied by the formation of metal-like clusters with $3D$-delocalized electrons [7, 8]. The electric conductivity of ES is determined primarily by the $1D$ hopping Mott transfer of electrons between these clusters and, to a lesser extent, by a more rapid $3D$ charge transfer inside the cluster. The electric conductivity of a cluster, calculated within the framework of the Drude model, amounts to $\sigma \geq 10^9$ S/m [9] and is comparable to that of *trans*-(poly(acetylene) [10]. However, the conductivity measured at a frequency of 6.5 GHz was equal only to $7 \times 10^4$ S/m [9], which implies that the actual pattern of electron transfer is masked by other processes that are difficult to study by the usual experimental techniques.

[1] This work was supported by the Russian Foundation for Basic Research, project no. 97-03-33707.

† Deceased.

Polarons in poly(aniline) possess unpaired electrons with the spin 1/2. In principle, we can, therefore, use the method of EPR spectroscopy to measure the diffusion of these paramagnetic centers both along a polymer chain and between the chains (with the coefficients $D_{1D}$ and $D_{3D}$, respectively) and study anisotropy of this mobility ($A = D_{1D}/D_{3D}$) within a few monomer units, even in unoriented polymer samples.

The value of $D_{1D}$ determined earlier by the EPR measurements at a comparatively low frequency proved to be $10^{12}$–$10^{14}$ rad/s and was weakly dependent on the doping level, while the $D_{3D}$ value was highly sensitive to $y$ and correlated with the conductivity of polymer samples measured by direct-current ($\sigma_{dc}$) and alternating-current ($\sigma_{ac}$) techniques [11]. This behavior was considered to be evidence for the existence of single highly conducting pathways with a $1D$ electron transfer between these channels. This interpretation is at variance with an alternative model based on the notion of $3D$ metal-like clusters formed in the doped polymer [7]. Therefore, the actual mechanism of charge transport in poly(aniline) is still the subject for discussion.

In the previous work [12], we demonstrated that passing to EPR measurements in the 2-mm waveband provides additional information about various condensed systems, including organic polymeric semiconductors [13, 14].

This article presents the results of our investigation into the magnetic and electron-transport properties of poly(aniline) samples with various doping levels. Using EPR measurements in the 2-mm waveband and a broad temperature range, we determined the relationships between the EPR signal shape and the composition, relaxation behavior, and mobility type of polarons in both forms of poly(aniline). A comparison of the $\sigma_{dc}$ and $\sigma_{ac}$ values allowed us to analyze the charge transfer mechanism and its dependence on the polymer doping level. Using the method of SHF saturation transfer, we succeeded in measuring the ultraslow librations of the polymer chain correlating with the interchain charge transfer. Preliminary results were reported in [15].

## EXPERIMENTAL

Emeraldin base (EB, sample I) in the powder form was synthesized by conventional method [16]. For obtaining ES samples with different preset doping levels $y$, the initial EB samples were exposed in a sulfuric acid solution with the corresponding pH value for two days, followed by drying in vacuum for 1 day. The doping level ($y$ = [S]/[N] = ~0.03 and 0.50 for samples II and III) was determined by elemental analysis.

The direct-current (dc) conductivity of the samples was measured by the four-point-probe (samples I and II) and two-point-probe (sample III) techniques in the temperature range 77–340 K.

The EPR measurements were performed on 2-mm [17]) and 3-cm (PS100X) spectrometers operated at a 100 kHz modulation frequency of the polarizing magnetic field. The total concentration of paramagnetic centers in the samples was determined by doubly integrating the EPR signals of a sample and a standard (evacuated ampule with a $10^{-3}$ M toluene solution of a stable nitroxyl radical 2,2,6,6-tetramethylpiperidinyloxyl). The **g** tensor components of the paramagnetic centers in the 2-mm waveband were determined by calibration with respect to the EPR spectra of a MgO powder with an admixture of $Mn^{2+}$ ions, adopting $g_{eff}$ = 2.00102 and $a$ = 8.74 mT. The determination errors of the peak-to-peak linewidth $\Delta B_{pp}$ and the $g$ values were $\pm 2 \times 10^{-3}$, $\pm 2 \times 10^{-4}$ mT in the 3-cm waveband and $\pm 5 \times 10^{-3}$, $\pm 3 \times 10^{-5}$ mT in the 2-mm waveband, respectively. The relaxation parameters of the paramagnetic centers in poly(aniline) samples were determined from their 2-mm dispersion spectra measured as described earlier [12, 18].

## RESULTS AND DISCUSSION

### *Relaxation and Dynamics of Polarons*

The 3-cm EPR spectrum of the paramagnetic centers in poly(aniline) exhibits a singlet signal with a Lorentzian lineshape. The EPR linewidth $\Delta B_{pp}$, depending on the temperature and the polymer doping level, amounts at room temperature to 1.13, 0.93, and 0.033 mT for samples I–III, respectively. Figure 1 shows the 2-mm EPR spectra of absorption and dispersion for samples I–III. Upon going from the 3-cm to the 2-mm waveband, the signal shape becomes Gaussian and the linewidth of samples I–III increases to $\Delta B_{pp}$ = 1.50, 1.31, and 0.16 mT, respectively, which is typical of organic polymeric semiconductors [12–14]. Here, the linewidth of samples I and II is virtually independent of the temperature, while that of sample III exhibits a A-shaped temperature dependence with an extremum at $T_e \approx 200$ K. The inphase and quadrature components of the 2-mm dispersion signal of samples I and II contain dome-shaped components (Fig. 1, spectra *b* and *c*), which reflect the fast adiabatic passage of individual saturated spin parcels.

The results of computer simulation showed that the 2-mm EPR spectra of the initial and slightly doped polymers represent a superposition of the spectra of radicals $R_1$ (Fig. 1, spectrum *a*) and $R_2$ stabilized, probably, in the amorphous and crystalline polymer phases, respectively. The $R_1$ radical has an anisotropic spectrum with the canonical **g** tensor components $g_{xx}$ = 2.00522, $g_{yy}$ = 2.00401, $g_{zz}$ = 2.00228, and the hyperfine coupling constant $A_{zz}$ = 2.27 mT. The $R_2$ radical signal is observed at $g_{\parallel}$ = 2.00223 and $g_{\perp}$ = 2.00463. Taking $A_{xx} = A_{yy}$ = 1.25 mT for paramagnetic centers in the pernigraniline base [19] and using the McConnell constant of hyperfine spin coupling to the nitrogen

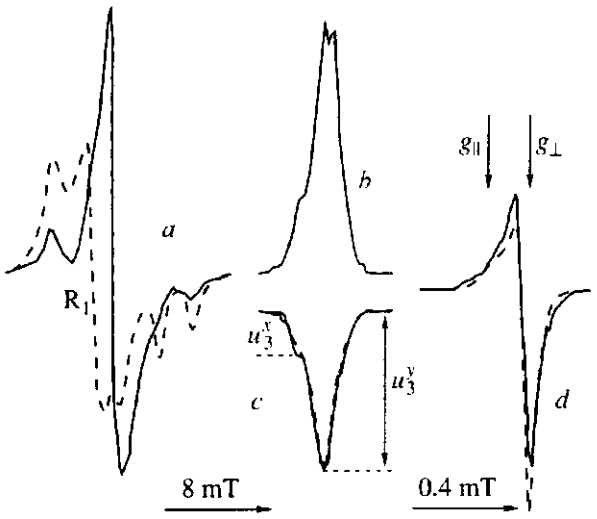


**Fig. 1.** Room-temperature (*a*, *d*) 2-mm waveband absorption spectra and the (*b*) inphase and (*c*) quadrature components of the 2-mm dispersion signal of samples (*a*–*c*) I, II and (*d*) III measured in an inert (He) atmosphere. Dashed lines show (*a*) the model spectrum of radical and (*c*, *d*) 2-mm waveband spectra measured at 200 K. Quantities $u_3^v$, $u_3^y$ (*c*) are the components of the quadrature dispersion signal; quantities $g_{\|}$, $g_{\perp}$ (*d*) are the **g**-tensor components of the $R_2$ radical.

nucleus ($Q_N$ = 2.37 mT [20]), we may calculate the spin density on the heteroatom by the formula $\rho_N^{\pi}(0) = (A_{xx} + A_{yy} + A_{zz})(3Q_N)$, which yields $\rho_N^{\pi} = 0.62$. Using the measured **g** tensor components, the $g$ value of free electron ($g_e$ = 2.00232), and the constant of spin–orbital electron coupling to the $^{14}N$ nucleus ($\lambda_N$ = 9.40 meV [21]), we may use the relation [20]

$$g_{xx,yy} - g_e = \frac{g_e \rho_N^{\pi} \lambda_N}{\Delta E_{1,2}} \qquad (1)$$

to calculate the energies of electron excitation to the nearest levels: $\Delta E_1$ = 3.77 eV and $\Delta E_2$ = 6.17 eV. The relative concentration of the $R_1$ radical in sample I at room temperature is $n_1/(n_1 + n_2)$ = ~0.3. This value decreases with decreasing temperature and/or increasing $y$. In the spectrum of sample III, the $R_2$ radical exhibits an axially-symmetric signal with $g_{\|}$ = 2.00361 and $g_{\perp}$ = 2.00338 (Fig. 1, spectrum *d*). It should be noted that a change of the inequality $g_{\|} < g_{\perp}$ to opposite upon doping the poly(aniline) is evidence for a reconstruction of the polymer crystal lattice in the course of the percolation process. Because the average $g$ value of the $R_1$ radical, $\langle g \rangle_1 = \frac{1}{3}(g_{xx} + g_{yy} + g_{zz})$ is approximately equal to that of the $R_2$ radical, $\langle g \rangle_2 = \frac{1}{3}(g_{\|} + 2g_{\perp})$, we may conclude that the $R_1$ radical represents a polaron localized in the polymer chain, while the $R_2$ radical is a polaron diffusing along the polymer chain at a minimum velocity [22]

$$\nu_{1D}^0 \geq \frac{(g_{xx} - g_e)\mu_B B_0}{2\pi\hbar}, \qquad (2)$$

where $\mu_B$ is the Bohr magneton, $B_0$ is the strength of external magnetic field, and $\hbar$ is the Planck constant. For a slightly doped ES sample this relation yields an estimate $\nu_{1D}^0 \geq 5.5 \times 10^7$ s$^{-1}$.

A decrease in the EPR linewidth upon doping can be related not only to the increase in the mobility of the charge carriers, but to a decrease in the spin density on the nitrogen nucleus and to a change in the polymer chain conformation as well. The transfer integral $I_{C\text{-}N}$ between the $p_z$ orbitals of nitrogen and carbon, occurring in the *para* position of the benzene rings of poly(aniline), depends on the dihedral angle as $I_{C\text{-}N} \sim \cos\theta$ and is inversely proportional to $\Delta E_i$, which is typical of aromatic hydrocarbons [23]. Assuming $\theta$ = 56° for EB [24], we can calculate the effective dihedral angle $\theta$ = 33° and the spin density on the nitrogen atom $\rho_N^{\pi}(0)$ = 0.42 by equation (1). This decrease in the $\theta$ value leads to the growth in the spin density on the benzene rings as a result of increase of the transfer integral $I_{C\text{-}N}$. Thus, the aforementioned variations in the magnetic parameters may be indicative of a more pronounced spin delocalization along the polymer chain and of a more planar chain conformation in ES as a result of doping.

An increase in the strength of the polarizing magnetic field leads to a significant decrease in the exchange interaction between spin parcels [25] and, hence, to an increase in the probability of their saturation in poly(aniline) (Fig. 1, spectra *b* and *c*). This effect was not previously observed in the EPR spectra of conducting polymers measured in lower magnetic fields. In the general case, an equation describing the first derivative of the dispersion signal $U$ can be written in the following form [26]:

$$U = u_1 \sin(\omega_m t) + u_2 \sin(\omega_m t - \pi) + u_3 \sin\left(\omega_m t - \frac{\pi}{2}\right), \qquad (3)$$

where $\omega_m$ is the angular frequency of modulation of the external magnetic field. The shape and intensity of the resulting signal depend on the times of spin–lattice ($T_1$) and spin–spin ($T_2$) relaxation of the paramagnetic centers. Because samples I and II obey the condition $\omega_m T_1 > 1$, their dispersion spectra are determined predominantly by the two last terms in equation (3) (Fig. 1,

spectra *b* and *c*, respectively). Figure 2 shows the temperature dependence of $T_1$ and $T_2$ for each of these samples determined separately from an analysis of components $u_2$ and $u_2$ of the dispersion spectra. The curves presented in Fig. 2 show evidence that the relaxation times approach one another with increasing doping level, because the interchain interaction increases as a result of the metal-like cluster formation.

Both intensity and shape of the dispersion signal may also depend on the ultraslow librational (torsional) reorientation of polarons localized in the polymer chain. This dynamics is usually studied by the method of SHF saturation transfer [27] based on introducing a stable radical with anisotropic magnetic parameter into the system studied, followed by measuring its saturated signal. Previously, we demonstrated that the saturation transfer measurements in the 2-mm waveband provide information about slow anisotropic reorientational molecular motions in highly viscous systems [12] such as conducting polymers [14]. The correlation time of librations about the *x*-axis of a polymer chain can be determined from equation [12]

$$\tau_c^x = \tau_0(u_3^x/u_3^y)^{-1.8} \quad (4)$$

where $\tau_0 = 7.9 \times 10^{-8}$. For the $R_1$ radical in EB (sample I), this equation yields $\tau_c^x = 3.1 \times 10^5 \exp[0.014\ \text{eV}/(k_B\ T)]$ s. A similar relation was obtained for sample II.

Interpretation of the electron relaxation data for samples I and II requires an assumption that polaron is capable of diffusing along the polymer chain and hopping from one chain to another. The spectral density function of this motion is as follows:

$$J(\omega_e) = n\phi(\omega_e)\Sigma_{ij}, \quad (5)$$

where $n = n_1 + n_2/\sqrt{2}$ is the effective number of $R_1$ and $R_2$ radicals with the concentrations per monomer unit $n_1$ and $n_2$, respectively. For a one-dimensional system, the Fourier image $\phi(\omega_e)$ is $(2D'_{1D}\,\omega_e)^{-1/2}$ for $D_{1D} > \omega_e > D_{3D}$ and $(2D'_{1D}D_{3D})^{-1/2}$ for $\omega_e \longrightarrow 0$ [28], where $D'_{1D} = 4D_{1D}N_p^{-2}$, $N_p$ is the spin delocalization length along the chain (expressed in monomer units), $\omega_e$ is the angular frequency of the spin precession, and $\Sigma_{ij}$ is the average lattice sum for the powder. Similar expressions for the spin density functions were used to study the spin dynamics in *trans*-poly(acetylene) and poly(aniline) [29, 30]. Taking into account that the electron relaxation is determined primarily by the dipole–dipole interaction of spins, we obtain the following equations for the electron relaxation rates [21, 31]:

$$T_1^{-1} = \langle\omega^2\rangle[2J(\omega_e) + 8J(2\omega_e)] \quad (6)$$

$$T_2^{-1} = \langle\omega^2\rangle[3J(0) + 5J(\omega_e) + 2J(2\omega_e)], \quad (7)$$

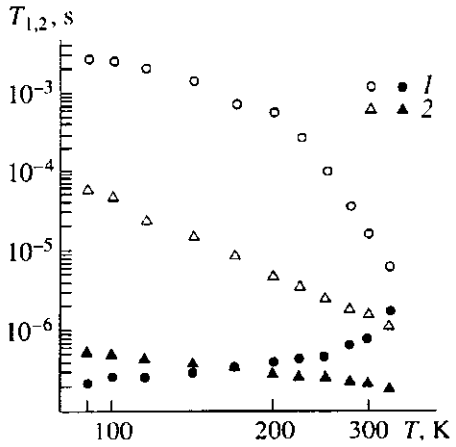


**Fig. 2.** Temperature dependence of the effective spin–lattice $T_1$ (open symbols) and spin–spin $T_2$ (black symbols) relaxation times for the paramagnetic centers in samples (*1*) I and (*2*) II.

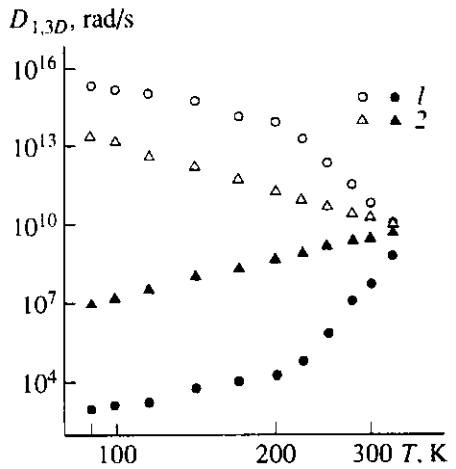


**Fig. 3.** Temperature dependence of the rates of paramagnetic center transfer along the chain (open symbols) and between the chains (black symbols) in samples (*1*) I and (*2*) II calculated by equations (6) and (7).

where $\langle\omega^2\rangle = 0.1(\mu_0/4\pi)^2\gamma_e^4\hbar^2S(S+1)n\Sigma_{ij}$ is the averaged constant of spin dipole interaction for the powder.

Figure 3 shows the temperature variation of the dynamic parameters $D_{1D}$ and $D_{3D}$ for samples I and II, calculated using the data of Fig. 2 and equations (6) and (7) for $N_p \approx 5$ [32]. As is seen, the value $D_{1D} \approx 5 \times 10^{11}$ rad/s calculated for $T = 300$ K is lower by two orders of magnitude when compared to the previously reported value for poly(aniline) with $y \approx 0.05$ [11], but yet significantly higher than the value $\nu_{1D}^0$ obtained above.

*Conductivity and Charge Transport in Neutral Poly(aniline)*

In contrast to *trans*-poly(acetylene) characterized by a typical temperature dependence of the conductivity $\sigma_{dc}(T) \sim T^{13.5}$ [5], EB exhibits a stronger variation with temperature: $\sigma_{dc}(T) \sim T^{22}$ for $T > 200$ K (Fig. 4). The slope of this curve is approximately equal to that of a similar function reported previously for EB in the high-temperature region [33] and cannot be interpreted within the framework of the Kivelson model of isoenergetic interchain polaron hopping [34]. At the same time, a qualitative analysis of this relationship within the framework of the Mott variable range hopping model for disordered semiconductors [35] leads to overstated values of the Mott parameters. Therefore, we may consider an alternative mechanism for the charge transfer in EB.

The high-frequency interchain conductivity of the initial EB sample can be calculated from the data presented in Fig. 3 by using the well-known relation

$$\sigma_{ac}(T) = \frac{Ne^2 D_{3D} b^2}{k_B T}, \quad (8)$$

where $N$ is the bulk concentration of mobile spin excitations and $b$ is the interchain spacing in the polymer. Figure 4 shows the temperature variation of $\sigma_{ac}$ calculated by equation (8) for $N = 9.5 \times 10^{23}$ m$^{-3}$ and $b = 0.439$ nm [36] in comparison with the relation $\sigma_{dc}(T) = 1.4 \times 10^{-64} T^{22}$ obtained for the EB sample in experiment. As is seen, the experimental and calculated curves vary in phase, at least at temperatures above 200 K. Apparently, the temperature dependence of the conductivity is described by two different functions $\sigma_{ac}(T)$ separated by a point of critical temperature $T_c = h\nu_{ph}/k_B \approx 200$ K, where $\nu_{ph} = 2k_F$ is the frequency of optical phonons. The total dependence can be explained by the range-dependent hopping of charge carriers for $T \le T_c$ and by the hopping dependent on both range and activation energy for $T \ge T_c$ (within the framework of the model of "small" polaron tunneling [37]). The latter model predicts the following relations for the high-frequency conductivity:

$$\sigma_{ac}(T) = \sigma_0 \left[ k_B T + \frac{4E_H}{\ln(2\nu_{ph}/\nu_e)} \ln\left(1 - \frac{k_B T}{E_H} \ln\frac{2\nu_{ph}}{\nu_e}\right)\right] \quad \text{for } T \le T_c \quad (9)$$

and

$$\sigma_{ac}(T) = \frac{\sigma_0}{k_B T} \exp\left(-\frac{E_a + E_H}{k_B T}\right) \quad \text{for } T \ge T_c, \quad (10)$$

where $E_H$ and $E_a$ are the hopping and activation energies, respectively.

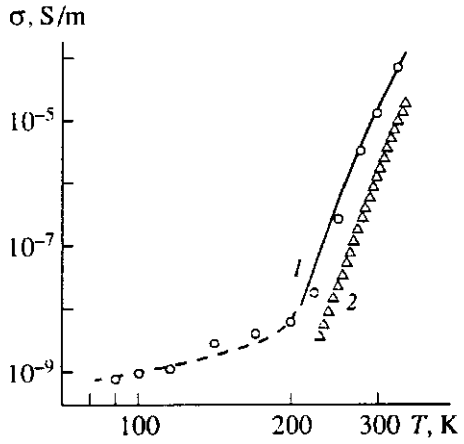


**Fig. 4.** Temperature variation of (*1*) the high-frequency conductivity of sample I determined using equation (8) for the data of Fig. 3 and (2) the experimental dc conductivity. Dashed line: calculation by equation (9) for $\sigma_0 = 1.3 \times 10^{-6}$ S/(m eV), $h\nu_{ph} = 0.017$ eV, and $E_H = 0.073$ eV; solid line: calculation by equation (10) for $\sigma_0 = 1450$ (S eV)/m, $E_H = 0.073$ eV, and $E_a = 0.40$ eV.

For comparison, Fig. 4 shows the temperature variation of $\sigma_{ac}$ calculated by equation (9) for $\sigma_0 = 1.3 \times 10^{-6}$ S/(m eV), $h\nu_{ph} = 0.017$ eV, $E_H = 0.073$ eV and by equation (10) for $\sigma_0 = 1450$ (S eV)/m, $E_H = 0.073$ eV, and $E_a = 0.40$ eV. As is seen, the experimental points fit easily into the calculated curves. Therefore, we may suggest that the charge transfer in this sample is provided predominantly by small mobile polarons. It must be noted that similar functions describing $\sigma_{ac}(T)$ were previously obtained for EB by conductometry at comparatively low frequencies [33] and for slightly doped poly(tetrathiafulvalen) by multifrequency EPR [12, 14, 37].

*Conductivity and Charge Transfer in Slightly Doped Poly(aniline)*

The charge transport in conducting organic polymers is determined by the interaction of charge carriers with optical phonons. This interaction modulates the resonance dimerization of *trans*-poly(acetylene) and the benzoid–quinoid transition in poly(*p*-phenylene) and some other conducting polymers. Kivelson [38] suggested that modulation of this type is also possible in the polymers with soliton-like nonlinear excitations. where the charge is transferred between the polaron–bipolaron pairs. This hypothesis was later confirmed for the slightly doped poly(*p*-phenylene) [39]. Thus, we may expect that the temperature dependence $\sigma_{dc}(T)$ and $\sigma_{ac}(T)$ in poly(aniline) will be similar to those calculated for *trans*-poly(acetylene) [34] and modified for poly(*p*-phenylene) and the like polymers [39]. The activation energy for the charge transfer between polarons is sufficiently low, because, similar to the case of intersoliton transfer, the system features a constant number

of polarons and bipolarons. In contrast to the case of *trans*-poly(acetylene), the polarons and bipolarons formed in other conducting polymers are charged. Taking this into account, the Kivelson equations for the dc and ac conductivity [34] can be written in the modified form [39]:

$$\sigma_{dc}(T) = \frac{k_1 e^2 \gamma(T) \xi \langle y \rangle}{k_B T N_i R_0^2} \exp\left(\frac{2k_2 R_0}{\xi}\right) = \sigma_0 T^m \quad (11)$$

$$\sigma_{ac}(T) = \frac{N_i^2 e^2 \langle y \rangle \xi_\parallel^3 \xi_\perp^2 \nu_e}{384 k_B T} \left[\ln \frac{2\nu_e}{\langle y \rangle \gamma(T)}\right]^4 = \frac{\sigma_0 \nu_e}{T} \left[\ln \frac{k_3 \nu_e}{T^{m+1}}\right]^4 \quad (12)$$

where $k_1 = 0.45$, $k_2 = 1.39$, and $k_3$ are constants; $\gamma(T) = \gamma_0(T/300\ \mathrm{K})^{m+1}$ is the velocity of charge transfer between polaron and bipolaron; $\langle y \rangle = y_p y_{bp}(y_p + y_{bp})^{-2}$, $y_p$ and $y_{bp}$ are numbers of polarons and bipolarons per monomer unit, respectively; $R_0 = (4\pi N_i/3)^{-1/3}$ is the average distance between dopant molecules; $N_i$ is the concentration of dopant molecules; $\xi = (\xi_\parallel \xi_\perp^2)^{1/3}$, $\xi_\parallel$, and $\xi_\perp$ are the spatially averaged, parallel, and perpendicular components of wavefunctions of the charge carriers, and $m \approx 10$. It is assumed that, unlike the case of neutral poly(aniline), the charge transfer in a slightly doped polymer is mediated by polarons of larger dimensions.

If the interpolaron charge transfer dominates in the total conductivity, the Kivelson theory predicts the relation $\sigma_{dc}(T) \sim T^m$ [equation (11)]. As is seen from Fig. 5, this law is valid, for example, in slightly doped poly(aniline). Therefore, we may conclude that the Kivelson law ($T^m$) provides a better description of the experimental dependence $\sigma_{dc}(T)$ for this sample than the Mott law ($T^{-1/2}$) does.

The concentration of mobile spins in sample II is $y_p = 1.1 \times 10^{-3}$ per pair of benzene rings. Taking into account the doubled charge on each bipolaron, we obtain for this sample $y_{bp} = 1.2 \times 10^{-2}$ and $\langle y \rangle = 7.9 \times 10^{-2}$. For the dopant concentration $N_i = 2.0 \times 10^{25}\ \mathrm{m}^{-3}$, we have $R_0 = 228$ nm. The value of $\gamma_0$ in equations (11) and (12) is $2.1 \times 10^{17}\ \mathrm{s}^{-1}$ as determined from $\sigma_{dc}(T)$. With an allowance for the spin delocalization over five monomer units [32] and the lattice constant $c_\parallel = 0.95$ nm [40], we obtain $\xi = 1.19$ nm. The perpendicular component $\xi_\perp$ of the quantity $\xi$ is determined from the equation $\xi_\perp = \frac{c_\perp}{\ln(\Delta_0/t_\perp)}$ [34], where $2\Delta_0$ is the bandgap width, $t_\perp = \frac{h^4 \nu_{3D} \nu_{ph}^3}{2\pi E_p} \exp\left(\frac{2E_p}{h\nu_{ph}}\right)$ [41], $h = 2\pi\hbar$, and $E_p$ is the energy of polaron formation. Assuming $2\Delta_0 = 3.8$ eV [42], $E_p = 0.1$ eV (typical of the π-conjugated polymers [41]), $\nu_\perp = 3.6 \times 10^8\ \mathrm{s}^{-1}$ (experimental value), and $\nu_{ph} = 4.2 \times 10^{12}\ \mathrm{s}^{-1}$, we obtain for sample II $t_\perp = 7.1 \times 10^{-3}$ eV, $\xi_\perp = 0.087$ nm, and $\xi = 0.21$ nm.

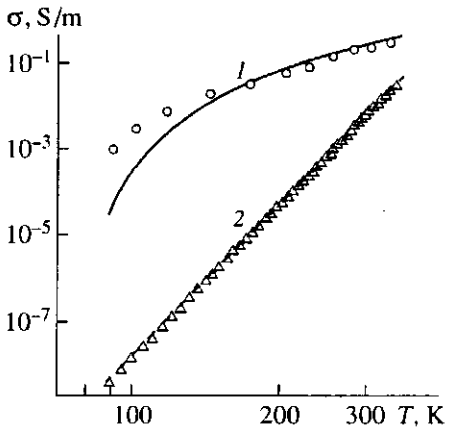


**Fig. 5.** Temperature variation of (*1*) the high-frequency conductivity of sample II determined using equation (8) for the data of Fig. 3 and (*2*) the experimental dc conductivity. Dashed and solid line show the results of calculation by equations (11) and (12), respectively, for $n = 12.1$, $\langle y \rangle = 0.081$, $\xi_\perp = 0.087$ nm, $\gamma_0 = 2.1 \times 10^{17}\ \mathrm{s}^{-1}$, $\xi_\parallel = 1.19$ nm, and $\nu_e = 140$ GHz.

Figure 5 presents the plot of $\sigma_{dc}(T) = 1.2 \times 10^{-36} T^{12.1}$ S/m calculated from equation (11) and the experimental data for sample II. For comparison, this figure also shows the function $\sigma_{ac}(T)$ calculated using equation (8) for $N = N_i$ and the data of Fig. 3, and the same function calculated by equation (11) for $m = 12.1$. As is seen from this figure, the experimental data can be described rather well within the framework of the Kivelson theory. Thus, the charge transfer by small polarons in the initial polymer is replaced by isoenergetic charge hopping between polaron and bipolaron. In polymer oxidized to a lesser extent, the charge transfer is probably described by superposition of the two mechanisms.

### *Conductivity and Charge Transfer in Ultimately Doped Poly(aniline)*

An analysis of the temperature dependence of the conductivity measured in the dc mode for sample III shows that the experimental data are described by the Mott law $\sigma_{dc}(T) = \sigma_0 \exp[-(T_0/T)^{1/2}]$ [35, 43], where $\sigma_0 = 1.8\nu_0 e^2 [n(\varepsilon_F) T_0/(\langle L \rangle T)]$; $\nu_0$ is the limiting hopping frequency; $T_0 = 16/[k_B n(\varepsilon_F) \langle L \rangle^3]$ is the percolation constant (or the effective distance between localized states) depending on the degree of disordering of the amorphous polymer regions; $\langle L \rangle = (L_\parallel L_\perp^2)^{1/3}$, $L_\parallel$, $L_\perp$ are the average length of the electron wavefunction and its

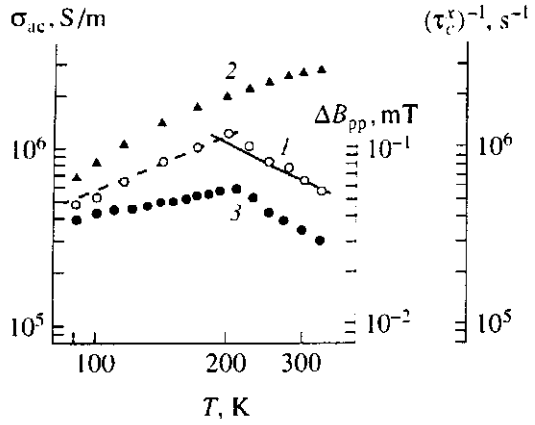


**Fig. 6.** Temperature variation of the high-frequency conductivity of sample I determined from asymmetry of the absorption spectrum (*1*, open circles) and calculated by equation (13) for $\langle L \rangle$ = 1.64 nm (*1*, dashed line) and equation (14) for $c$ = 0.950 and $\alpha$ = 41 eV/nm (*1*, solid line). For the comparison, dark symbols show the plots of (2) $\tau_c^x(T) = 3.1 \times 10^{-5}\exp[0.014\ \text{eV}/(k_B T)]$ calculated for sample I by equation (4) and (*3*) $\Delta B_{pp}(T)$ values determined for sample III from 3-cm waveband EPR absorption spectra.

projections in the parallel and perpendicular directions. Using the slope of the $\sigma_{dc}(T)$ curve and the value $n(\varepsilon_F) = 3.8\ \text{eV}^{-1}\ \text{mol}^{-1}$ for sample III, we obtain $T_0$ = 1650 K and $\langle L \rangle$ = 1.92 nm. The values of $L_\parallel$ 7.0 and $L_\perp$ 1.0 nm were determined as described in [44]. The frequency $\nu_0$ equals approximately $3.4 \times 10^{12}\ \text{s}^{-1}$, which is sufficiently close to $\nu_0 = 1.6 \times 10^{13}\ \text{s}^{-1}$ reported previously for ES [8]. Thus, the frequency of the lattice phonons determined from the relation $\nu_{ph} = k_B T_c/h$ is $4.2 \times 10^{12}\ \text{s}^{-1}$, which is close to the calculated value of $\nu_0$.

In a doped polymer, the dipole–dipole interaction between spin parcels increases significantly and the effective relaxation time of the paramagnetic centers decreases markedly. This accounts for the reduced sensitivity of the saturation methods with respect to the spin relaxation and dynamics. The mobility of the charge carriers can be determined by the analysis of an absorption spectrum containing the Dyson component using a relation for the skin layer thickness (see, e.g., [45–47]) $\delta = \dfrac{c}{2\pi\sqrt{\nu_e \sigma_{ac}}}$, where $c$ is a constant. Such a component appears in the absorption spectrum of sample III (Fig. 1, spectrum *d*). Therefore, once the average size of the metal-like clusters in the sample is known, we can determine their 3*D* conductivity $\sigma_{ac}$.

Figure 6 shows the plot of $\sigma_{ac}(T)$ for the metallike clusters in sample III. As is seen, the maximum conductivity $\sigma_{ac} = 1.2 \times 10^6$ S/m (reached at $T = T_c$) is higher by almost two orders of magnitude when compared to a similar quantity for the ultimately doped ES measured at 6.5 GHz [9].

The form of this function is indicative of a 1*D* localization of electron (semiconductor regime) at $T \le T_c$ and a 3*D* localization (metal regime) in clusters formed at higher temperatures. It should be noted that similar behavior was observed earlier for the thermo emf and the spin diffusion coefficient $D_{1D}$ in ES in the same temperature range [8, 48].

An analysis of the $\sigma_{ac}$ curves presented in Fig. 6 shows that the conductivity of clusters at $T \le T_c$ obeys the Mott law [35, 43]

$$\sigma_{ac}(T) = \frac{2}{3}\pi^2 e^2 k_B T n^2(\varepsilon_F)\langle L \rangle^5 \nu_e \left[\ln\frac{\nu_0}{2\pi\nu_e}\right]^4, \quad (13)$$

while the process at $T \ge T_c$ is determined by the scattering of charge carriers on the optical lattice phonons. In this case, the theory of charge transport for the conducting polymers yields [10.49]

$$\sigma_{ac} = \frac{e^2 \nu_{ph} M t_0^2}{\hbar^2 c_\parallel \alpha^2}\sinh\left(\frac{h\nu_{ph}}{k_B T}\right), \quad (14)$$

where $M$ is the mass of the CH group, $c_\parallel$ is the lattice constant, and $\alpha$ is the spin–phonon interaction constant. As is seen from Fig. 6, the experimental values of $\sigma_{ac}(T)$ are described well by functions of the type (13) and (14) for $\langle L \rangle$ = 1.64 nm; $c_\parallel$ = 0.95 nm [40], and $\alpha$ = 41 eV/nm [10]. Thus, we may conclude that the charge carriers in ultimately doped ES at low temperatures are transferred by the mechanism of variable range hopping between polymer chains and scattered on the lattice phonons when the phonon energy becomes comparable with $k_B T_c$. The conductivity of metallike clusters calculated for *trans*-poly(acetylene) and ES was approximately $10^8$ and $10^9$ S/m, respectively [9, 10]. However, according to our data, this level of conductivity can be reached only if the mass of monomer units exceeds that of CH by two orders of magnitude.

The spin and charge dynamics in poly(aniline) must also depend on the librational motions of macromolecules modulating the spin–spin interaction and the transfer integral, similar to the organic crystalline semiconductors [50]. Figure 6 shows the correlation between the $\sigma_{ac}(T)$ plots for the ES sample and $\tau_c^x(T)$ values for a slightly doped ES sample, at least for $T \le T_c$. Assuming that the polymer chain dynamics does not change significantly upon doping, we concluded that the librational vibrations of the lattice actually modulate the spin exchange interactions and the charge transfer integral. Because the charge carriers are surrounded by electron and phonon shells, we may sug-

gest that the spin relaxation and charge transfer are be accompanied by the absorption of a certain number of phonons. These joint electron–phonon processes are apparently dominating in doped polymers with strongly interacting chains constituting the $3D$ metallike clusters.

Because the velocity of charge carriers near the Fermi surface of an ultimately doped ES sample, $v_F = 4c_{\parallel}/[hn(\varepsilon_F)]$, is about $2.5 \times 10^5$ m/s. the corresponding value of the diffusion coefficient for the charge transfer between polymer chains is $D_{3D} = v_F/L_\perp = 2.4 \times 10^{14}$ rad/s. Equation (8) gives $\sigma_{ac} = 1.3 \times 10^6$ S/m for $b = L_\perp = 1.0$ nm and $T_c \approx 200$ K. This estimate is close to the conductivity of ES determined from an analysis of the shape of the EPR spectrum of this sample, which is additional evidence for the existence of metallike cluster with $3D$-delocalized electrons. Similarly to the case of classical metals, we can calculate the effective mass of charge carriers $m^* = (3\pi^2 N)^{-1/3} h v_F^{-1}$ [51], which proves to be about twice the mass of free electron, and their mean free path $l_i = \sigma_{ac} m^* v_F/(Ne^2)$ [51], equal to 8.0 nm for this sample at $T = T_c$. The latter value is somewhat smaller compared to the mean free path of solitons in oriented *trans*-poly(acetylene) [10, 52], but yet sufficiently long for the ES to be considered an organic metal with distributed electron states.

## CONCLUSION

In a neutral undoped poly(aniline), the charge is transferred by small polarons, for which the probability of interchain hopping is dependent significantly on the energy of the lattice phonons. In a slightly doped poly(aniline), a comparatively narrow energy distribution of charge carriers (of the order of $k_BT$) leads to dominating isoenergetic charge transfer. As a result, the conductivities $\sigma_{dc}(T)$ and $\sigma_{ac}(T)$are determined by the interaction of polarons and bipolarons with charged dopant molecules and are described within the framework of the Kivelson model. This agrees with the notions of intersoliton charge hopping in the slightly doped poly(aniline). At a greater doping level, the energy distribution width of charge carriers exceeds $k_BT$, and the charge is transferred predominantly by the mechanism of variable range hopping between chains.

Doping of the polymer leads to the formation of massive metallike clusters, which is accompanied by a significant increase in the intensity of both electron–phonon and interchain interactions. The latter factor plays a role in the pinning of the metallike state suppressing the $1D$ localization and the Peyers instability in poly(aniline). The charge transfer in metallike ES clusters is modulated by ultraslow librational motions of the polymer chains. The metallike clusters are composed of packed polymer chains characterized by $3D$-delocalization of the conduction electrons, which contradicts the concept of single conducting pathways in ES.

## ACKNOWLEDGMENTS

The authors are grateful to B.Z. Lubentsov for kindly providing the ES samples and to A.S. Astakhova for performing the elemental analysis of the samples.

## REFERENCES

1. *Electronic Properties of Polymers*, Kuzmany, H., Mehring, M., and Roth, S., Eds., Berlin: Springer, 1992.
2. *Proc. Intern. Conf. on Science and Technology of Synthetic Metals (ICSM'96)*. Snowbird, USA, 1996.
3. Heeger, A.J., *Handbook of Conducting Polymers*, Scotheim, T.A., Ed., New York: Marcel Dekker, 1986, vol. 2, p. 729.
4. Chance, R.R., Boudreaux, D.S., Brédas, J.L., and Silbey, R., *Handbook of Conducting Polymers*, Scotheim, T.A., Ed., New York: Marcel Dekker, 1986, vol. 2, p. 825.
5. Epstein, A.J., *Handbook of Conducting Polymers*, Scotheim, T.A., Ed., New York: Marcel Dekker, 1986, vol. 2, p. 1041.
6. McCall, R.P., Ginder, J.M., Roe, M.G., Asturias, G.E., Scherr, E.M., VacDiarmid, A.G., and Epstein, A.J., *Phys. Rev. B: Condens. Matter*, 1989, vol. 39, no. 14, p. 10174.
7. Wang, Z.H., Ray, A., MacDiarmid, A.G., and Epstein, A.J., *Phys. Rev. B: Condens. Matter*, 1991, vol. 43, no. 5, p. 4373.
8. Wang, Z.H., Scherr, E.M., MacDiarmid, A.G., and Epstein, A.J., *Phys. Rev. B: Condens. Matter*, 1992, vol. 45, p. 4190.
9. Joo, J., Oh, E.J., Min, G., MacDiarmid, A.G., and Epstein, A.J., *Synth. Met.*, 1995, vol. 69, nos. 1–3, p. 251.
10. Kivelson, S. and Heeger, A.J., *Synth. Met.*, 1988, vol. 22, p. 371.
11. Mizoguchi, K., Nechtschein, M., Travers, J.-P., and Menardo, C., *Phys. Rev. Lett.*, 1989, vol. 63, no. 1, p. 66.
12. Krinichnyi, V.I., *The 2-mm Waveband EPR Spectroscopy of Condensed Systems*, Boca Raton: CRC, 1995.
13. Krinichnyi, V.I., *Usp. Khim.*, 1996, vol. 65, no. 1, p. 84.
14. Krinichnyi, V.I., *Usp. Khim.*, 1996, vol. 65, no. 6, p. 564.
15. Krinichnyi, V.I., Chemerisov, S.D., and Lebedev, Ya.S., *Synth. Met.*, 1997, vol. 84, nos. 1–3, p. 819.
16. Timofeeva, O., Lubentsov, B., Sudakova, Ye., Chernyshov, D., and Khidekel, M., *Synth. Met.*, 1991, vol. 40, no. 1, p. 111.
17. Galkin, A.A., Grinberg, O.Ya., Dubinskii, A.A., Kabdin, N.N., Krymov, V.N., Kurochkin, V.I., Lebedev, Ya.S., Oranskii, L.G., and Shuvalov, V.F., *Prib. Tekh. Eksperim.*, 1977, no. 4, p. 284.
18. Pelekh, A.E., Krinichnyi, V.I., Brezgunov, A.Yu., Tkachenko, L.I., and Kozub, G.I., *Vysokomol. Soedin., Ser. A*, 1991, vol. 33, no. 8, p. 1731.
19. Long, S.M., Cromack, K.R., Epstein, A.J., Sun, Y., and MacDiarmid, A.G., *Synth. Met.*, 1993, vol. 55, no. 1, p. 648.

20. Buchachenko, A.L. and Vasserman, A.M., *Stabil'nye radikaly* (Stable Radicals), Moscow: Khimiya, 1973.
21. Carrington, F. and McLachlan, A.D., *Introduction to Magnetic Resonance with Application to Chemistry and Chemical Physics*, New York: Harper and Row, 1967.
22. Pool, Ch.P., *Electron Spin Resonance: A Comprehensive Treasure on Experimental Techniques*, New York: Wiley, 1983.
23. Traven', V.F., *Elektronnaya struktura i svoistva organicheskikh molekul* (Electron Structure and Properties of Organic Molecules), Moscow: Khimiya, 1989.
24. Masters, J.G., Ginder, J.M., MacDiarmid, A.G., and Epstein, A.J., *J. Chem. Phys.*, 1992, vol. 96, no. 6, p. 4768.
25. Al'tshuler, S.A. and Kozyrev, B.M., *Elektronnyi paramagnitnyi rezonans soedinenii elementov promezhutochnykh grupp* (Electron Paramagnetic Resonance of Transition Element Compounds), Moscow: Nauka, 1972.
26. Gullis, P.R., *J. Magn. Reson.*, 1976, vol. 21, no. 3, p. 397.
27. Hyde, J.S. and Dalton, L.R., *Spin Labeling. Theory and Application*, London: Academic, 1979, vol. 2, p. 1.
28. Butler, M.A., Walker, L.R., and Soos, Z.G., *J. Chem. Phys.*, 1976, vol. 64, p. 3592.
29. Nechtschein, M., Devreux, F., Genoud, F., Gugleielmi, M., and Holczer, K., *Phys. Rev. B: Condens. Matter*, 1983, vol. 27, no. 1, p. 61.
30. Mizoguchi, K., *Makromol. Chem., Macromol. Symp.*, 1990, vol. 37, p. 53.
31. Abragam, A., *The Principles of Nuclear Magnetism*, Oxford: Clarendon, 1961.
32. Devreux, F., Genoud, F., Nechtschein, M., and Villeret, B., *Electronic Properties of Conjugated Polymers*, Kuzmany, H., Mehring, M., and Roth, S., Eds., Berlin: Springer, 1987, p. 270.
33. Zuo, F., Angelopoulos, M., MacDiarmid, A.G., and Epstein, A.J., *Phys. Rev. B: Condens. Matter*, 1989, vol. 39, no. 6, p. 3570.
34. Kivelson, S., *Phys. Rev. B: Condens. Matter*, 1982, vol. 25, no. 6, p. 3798.
35. Mott, N.F. and Davis, E.A., *Electronic Processes in Non-Crystalline Materials*, Oxford: Clarendon, 1979.
36. Lubentsov, B.Z., Timofeeva, O.N., Saratovskikh, S.V., Krinichnyi, V.I., Pelekh, A.E., Dmitrenko, V.I., and Khidekel, M.L., *Synth. Met.*, 1992, vol. 47, no. 1, p. 187.
37. Patzsch, J. and Gruber, H., *Electronic Properties of Polymers*, Kuzmany, H., Mehring, M., and Roth, S., Eds., Berlin: Springer, 1992, p. 121.
38. Kivelson, S., *Mol. Cryst. Liq. Cryst. Sci. Technol., Sect. A*, 1981, vol. 77, no. 1, p. 65.
39. Kuivalainen, P., Stubb, H., Isotalo, H., Yli-Lahti, P., and Holmström, C., *Phys. Rev. B: Condens. Matter*, 1985, vol. 31, no. 12, p. 7900.
40. Jozefowicz, M.E., Laversanne, R., Javadi, H.H.S., Epstein, A.J., Pouget, J.P., Tang, X., and MacDiarmid, A.G., *Phys. Rev. B: Condens. Matter*, 1989, no. 17, p. 12958.
41. Zuppiroli, L., Paschen, S., and Bussac, M.N., *Synth. Met.*, 1995, vol. 69, nos. 1–3, p. 621.
42. Cao, Y., Li, S., Xue, Z., and Guo, D., *Synth. Met.*, 1986, vol. 16, p. 305.
43. Nakhmedov, E.P., Prigodin, V.N., and Samukhin, A.N., *Fiz. Tverd. Tela*, 1989, vol. 31, no. 3, p. 64.
44. Wang, Z.H., Javadi, H.H.S., Ray, A., MacDiarmid, A.G., and Epstein, A.J., *Phys. Rev. B: Condens. Matter*, 1990, vol. 42, no. 8, p. 5411.
45. Goldberg, I.B., Crowe, H.R., Newman, P.R., Heeger, A.J., and MacDiarmid, A.G., *J. Chem. Phys.*, 1979, vol. 70, no. 3, p. 1132.
46. Elsenbaumer, R.L., Delannoy, P., Muller, G.G., Forbes, C.E., Murthy, N.S., Eckhardt, H., and Baughman, R.H., *Synth. Met.*, 1985, vol. 11, no. 4/5, p. 251.
47. Cosmo, R. and Dormann, E., Gotschy, B., Naarmann, H., and Winter, H. *Synth. Met.*, 1991, vol. 41, no. 1/2, p. 369.
48. Mizoguchi, K. and Kume, K., *Synth. Met.*, 1995, vol. 69, nos. 1–3, p. 241.
49. Pietronero, L., *Synth. Met.*, 1983, vol. 8, no. 2, p. 225.
50. Silin'sh, E.A., Kurik, M.V., and Chapek, V., *Elektronnye protsessy v organicheskikh molekulyarnykh kristallakh: yavleniya lokalizatsii i polyarizatsii. Riga* (TRaNSl): Zinatne, 1988.
51. Blakemore, G.S., *Solid State Physics*, Cambridge: Cambridge Univ., 1985.
52. Javadi, H.H.S., Chakraborty, A., Li, C., Theophilou, N., Swanson, D.B., MacDiarmid, A.G., and Epstein, A.J., *Phys. Rev. B: Condens. Matter*, 1991, vol. 43, no. 3, p. 2183.